

On the Mesomorphic Form of Poly(ethylene terephthalate)

Finizia Auriemma, Paolo Corradini, Claudio De Rosa, Gaetano Guerra,* and Vittorio Petraccone

Dipartimento di Chimica, Università di Napoli Federico II, via Mezzocannone, 4, 80134 Napoli, Italy

Riccardo Bianchi and Gabriele Di Dino

*Centro Ricerche Montefibre, 80011 Acerra, Napoli, Italy**Received July 31, 1991; Revised Manuscript Received December 11, 1991*

ABSTRACT: The conformation and the packing of poly(ethylene terephthalate) (PET) chains in the mesomorphic form have been investigated by accurate X-ray diffraction measurements, conformational energy analysis, and calculations of Fourier transforms of models. The X-ray diffraction pattern presented here is richer than those previously reported. In particular, besides the known meridional peaks at $\zeta = 1/c$ and $3/c$, corresponding to a periodicity of 10.3 Å, a stronger meridional peak at $\zeta = 5/c$ has been shown. The reported Fourier transform calculations of isolated-chain models indicate that the experimental diffraction pattern of the mesomorphic form of PET can be qualitatively accounted for by extended linear chains obtained by random sequences of monomeric units in different minimum energy conformations. These random sequences of monomeric units generate chains in which any long-range correlation between the planes of the phenylene rings, along the chain, is absent.

Introduction

A mesomorphic form of poly(ethylene terephthalate) (PET) was found several years ago by Bonart.¹⁻³ It can be obtained by drawing procedures on amorphous unoriented samples at temperatures below the glass transition (T_g), and it is transformed into the usual triclinic structure by heating above T_g .

Photographic X-ray diffraction patterns of this form, although not always recognized, have been reported in several papers.³⁻⁷ The reported patterns present only two crystalline reflections on the meridian, with a spacing of 10.3 Å,⁴ which is different from the spacing of the corresponding meridional reflections (10.7 Å) observed for the usual triclinic form.^{8,9} Besides the meridional reflections, only a very broad (with respect to both reciprocal coordinates ξ and ζ) scattering peak on the equator is present.⁴

It is, possibly, worth noting that there are other papers dealing with "mesomorphic regions" or with an "intermediate phase" for PET which would be present in semicrystalline fibers containing the triclinic form.¹⁰⁻¹³ In particular, possible techniques for the evaluation of the amount of this intermediate form from X-ray diffraction patterns of oriented samples have been described^{10,11} and used.^{12,13} This intermediate phase is an anisotropic amorphous phase which does not correspond to the mesomorphic form considered in this paper and in refs 1-7. In fact, this amorphous oriented phase would be largely present also in conditions for which the mesomorphic form is absent (e.g., for samples annealed at 140 °C¹² or even at 220 °C¹³). We recall that the peaks typical of the mesomorphic form completely disappear for annealing of the fibers above 100 °C.¹⁴

Only one detailed model for the mesomorphic form of PET has been proposed.⁴ It is based on a division of the broad equatorial peak into four peaks and on possible analogies with the structure of the triclinic form and consists of a paracrystalline monoclinic structure ($a = 4.9$ Å, $b = 9.2$ Å, $c = 10.5$ Å, $\alpha = 100^\circ$).⁴ In particular, a tilt angle of the c -axis of about 10° with respect to the draw axis was assumed so that the spacing of the meridional reflections of 10.3 Å would correspond to a chain repetition

of 10.5 Å. The reduction of the chain repetition, in comparison with the value found for the triclinic form (10.7 Å), was attributed to some undefined shrinkage of the polymer conformation.

This model, however, can be subjected to a major criticism. In fact, it does not consider the occurrence of some conformational disorder in the polymer chains, which is, instead, clearly suggested by the absence of the meridian of diffracted intensity confined to layer lines.

In this contribution, the conformation and the packing of PET chains in the mesomorphic form are investigated by X-ray diffraction measurements, conformational energy analysis, and calculation of Fourier transforms of models. In the Experimental Section the X-ray diffraction pattern of a sample in the mesomorphic form, collected by an automatic diffractometer, is presented, thus providing quantitative and more complete information relative to the diffracted intensity. In the next section energy calculations as well as geometrical considerations relative to isolated-chain models of PET are presented. The aim is to find possible ordered and disordered conformations presenting average periodicities close to that one experimentally observed for the mesomorphic form of PET (10.3 Å). In the final section of the paper, the possible validity for the mesomorphic form of models, characterized as geometrically and energetically feasible, has been tested through comparisons between the corresponding calculated Fourier transforms and the experimental diffraction intensity.

Experimental Section

PET pellets with an intrinsic viscosity of 0.78 dL/g were supplied by Montefibre S.p.A. Samples of PET in the mesomorphic form were obtained by suitable thermomechanical treatment of monofilaments extruded at 280 °C having a thickness of 0.5 mm. Monofilaments of nearly 8-mm length were drawn at room temperature with a draw ratio close to 4 at a speed of 5 mm/min and then annealed at 60 °C for 1 h. Samples in the mesomorphic form with similar X-ray diffraction patterns have been, however, obtained by analogous treatment of industrial multifilament spun yarns with an intrinsic viscosity of 0.64 dL/g.

The X-ray diffraction patterns for stretched fibers were obtained by using a Nonius automatic X-ray diffractometer with

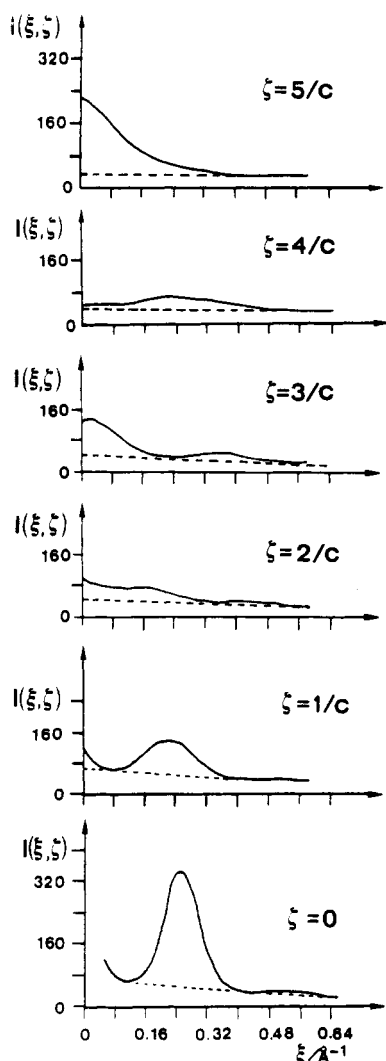


Figure 1. Experimental X-ray diffraction intensity (arbitrary units) of PET in the mesomorphic form vs ξ for the equator and layer lines corresponding to a periodicity of $c = 10.3 \text{ \AA}$. Dashed lines put in evidence the background scattering.

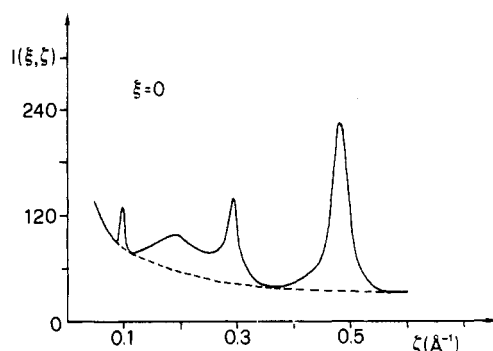


Figure 2. Experimental X-ray diffraction intensity (same units as in Figure 1) of PET in the mesomorphic form on the meridian. Dashed line shows the background scattering.

Ni-filtered $\text{Cu K}\alpha$ radiation and were collected always maintaining an equatorial geometry in the range of $0 < \zeta < 0.6 \text{ \AA}^{-1}$ at intervals of 0.0097 \AA^{-1} and the range of $0 < \xi < 0.6 \text{ \AA}^{-1}$ at intervals of 0.01 \AA^{-1} .

The diffraction intensities ($I(\xi, \zeta)$) as collected along the equator and the layer lines with $\zeta = l/c$ (l integer ≤ 5) corresponding to a periodicity of $c = 10.3 \text{ \AA}$ are plotted in Figure 1 vs the reciprocal coordinate ξ . The diffracted intensity on the meridian (that is, the intensity at $\xi = 0$ for variable values of ζ) is reported in Figure 2. Dashed lines in Figures 1 and 2 show the background scattering.

The decimal logarithm of the diffracted intensities after subtraction of the background and correction by the Lorentz

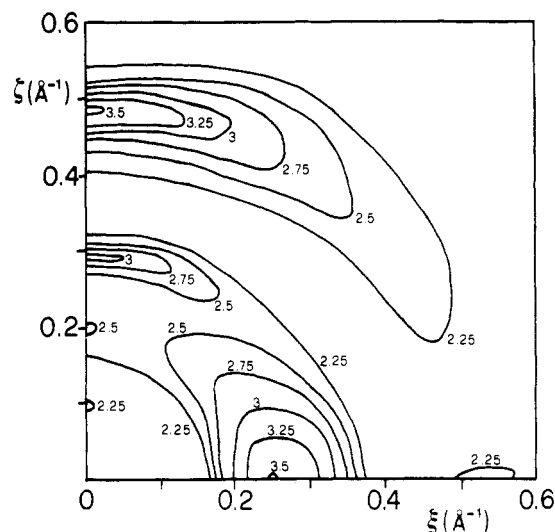


Figure 3. Decimal logarithm of the corrected experimental X-ray diffraction intensity $I(\xi, \zeta)$ of poly(ethylene terephthalate) in the mesomorphic form vs reciprocal coordinates ξ and ζ . The background has been subtracted from the X-ray diffraction intensity, which was hence corrected by the Lorentz and polarization factors. Contour lines with constant $\log [I(\xi, \zeta)]$ values are at regular intervals of 0.25 , $\log [I(0, 3/c)]$ being placed equal to 3 .

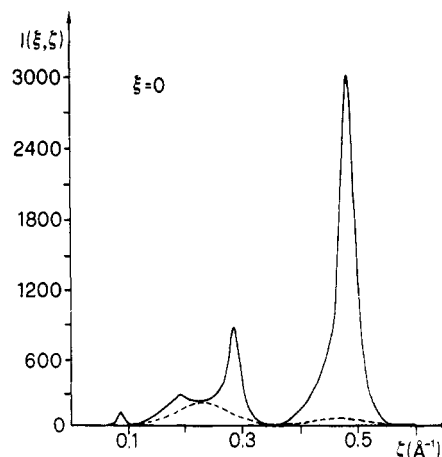


Figure 4. Experimental X-ray diffraction intensity of PET in the mesomorphic form on the meridian, subtracted for the background and corrected by the Lorentz and polarization factors. $I(0, 3/c) = 1000$. The dashed line indicates a tentative evaluation of the contribution from the unoriented amorphous material.

and polarization factors (Lp) (which according to the diffraction geometry is $Lp = (1 + \cos^2 2\theta)/\sin 2\theta$) is reported in Figure 3 as a function of the reciprocal coordinates ξ and ζ . The corrected diffracted intensity on the meridian is shown in Figure 4. In both Figures 3 and 4, $I(0, 3/c)$ has been fixed equal to 1000 .

The presence of three well-defined meridional "reflections" for $\zeta = 0.096 \text{ \AA}^{-1}$, $\zeta = 0.29 \text{ \AA}^{-1}$, and $\zeta = 0.48 \text{ \AA}^{-1}$ is apparent, indicating, in agreement with previous measurements,⁴ a periodicity along the chain of 10.3 \AA . Only a broad meridional halo is present around $\zeta = 2/c = 0.194 \text{ \AA}^{-1}$. It is worth noting that in the region $0.12 < \zeta < 0.30 \text{ \AA}^{-1}$ there is a substantial contribution from un-oriented amorphous material. This contribution is roughly drawn in Figure 4. Off the meridian, besides the strong and very broad equatorial peak, there are, substantially, only two halos corresponding to the two strong meridional peaks.

The experimental data allow us to state the following: (i) the diffuse equatorial diffraction peak centered at $d = 4.0 \text{ \AA}$ (spanning $3.2 < d < 5.0 \text{ \AA}$) mainly gives information about the mean distance between the centers of mass of adjacent polymer chains; (ii) the absence of diffraction peaks off the meridian suggests that in the mesomorphic form of PET correlations in the positions and orientations of the chains, besides a nearly parallel placement of

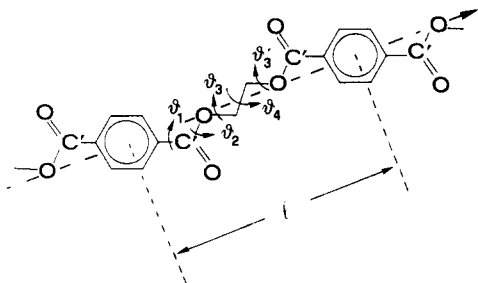


Figure 5. Labeling scheme used to define atoms and bond parameters.

Table I
Values of Bond Lengths and Valence Angles Used in the Calculations of the Conformational Energy and of the Geometrical Features of PET^a

bond lengths, Å	bond angles, deg
C _{Ph} –C _{Ph} = 1.39	τ(C _{Ph} C _{Ph} C _{Ph}) = 120
C _{Ph} –C' = 1.48	τ(C _{Ph} C _{Ph} C') = 120
O–C' = 1.34	τ(C _{Ph} C'O) = 124
O=C' = 1.21	τ(C _{Ph} C'O) = 113
C–O = 1.45	τ(C'OC) = 116, 111 ^b
C–C = 1.50	τ(OCC) = 106

^a Obtained by averaging the crystallographic data of PET in the triclinic form⁹ and of low molecular weight model compounds.^{14,15}

^b In the calculations, τ(C'OC) = 111° when θ₃ is in a gauche state and τ(C'OC) = 116° when θ₃ is in the trans state.^{9,14–16}

the chain axes, are substantially absent; (iii) the substantial absence of layer lines (off the meridian) suggests also that in the mesomorphic form conformationally disordered chains are packed; and (iv) the broadness along ζ of the meridional reflections indicates an average coherent length along the chain axis of the order of 80 Å.

Conformational Analysis

Methods. The calculations of the conformational energy have been performed on the portion of the chain shown in Figure 5, where the labeling scheme used to define atoms and bond parameters is also indicated.

The energy and geometric analyses have been performed keeping, for the sake of simplicity, bond lengths and valence angles fixed. Their values, listed in Table I, are generally taken from structural data of PET^{8,9} and of low molecular weight model compounds.^{14,15} For the τ(C'OC) bond angle, two different values have been assumed, τ(C'OC) = 111°, when θ₃ is in the gauche state (on the basis of structural data of poly(tetramethylene terephthalate) in the α form¹⁶), or τ(C'OC) = 116°, when θ₃ is in the trans state (from structural data of PET^{8,9}). However, only calculations assuming τ(C'OC) = 111° are reported.

The conformational energy is given by the sum of the terms

$$E = E_{\text{tor}} + E_{\text{nb}} + E_{\text{el}} \quad (1)$$

where E_{tor} is the sum of the energy contributions associated with torsion angles (θ) around single bonds, evaluated by terms of the kind

$$E_{\text{tor}} = (K_T/2)(1 + \cos n\theta) \quad (2)$$

with barrier height K_T and n depending on the kind of bond; E_{nb} is the sum of the energy contributions due to the interactions between atoms separated by more than two bonds, evaluated by terms of the kind

$$E_{\text{nb}} = Ar^{-12} - Br^{-6} \quad (3)$$

with r the interatomic distance and A and B the repulsive and attractive constants, respectively; and E_{el} is the sum

of the energy contributions due to interatomic electrostatic interactions, evaluated by terms of the kind

$$E_{\text{el}} = (1/\epsilon)qq'/r \quad (4)$$

with q and q' the electrostatic charges associated with atoms at distance r and ϵ the dielectric constant.

The torsion barrier for the θ₄ dihedral angles has been assumed threefold (minima corresponding to the trans, gauche⁺ and gauche[−] states) and equal to 2.8 kcal/mol.¹⁷ An inherent torsional potential for θ₃ was not included in the calculations owing to the low torsion barrier.^{17,18} The torsion barrier for the θ₂ dihedral angles has been assumed twofold and equal to 8.75 kcal/mol.¹⁸ Finally, the torsion barrier for the θ₁ dihedral angles has been assumed twofold and equal to 5.0 kcal/mol.¹⁹

For the nonbonded interactions Scheraga's set²⁰ of parameters was used. The energy parameters for the oxygen O_{sp}³ and for the carbon atoms of the phenylene rings used with Scheraga's set have been obtained assuming, in order, the following values of polarizability, effective number of electrons, and van der Waals radii: for O_{sp}³ 0.7 Å³, 7,²¹ and 1.5 Å;²² for the aromatic carbon atoms 1.23 Å³, 5,²³ and 1.8 Å.²⁴ Values of B for the various couples of interacting atoms were calculated from polarizabilities and effective number of electrons as detailed in ref 21. The values of A were selected in such a way as to make a minimum when r is the sum of the adjusted van der Waals radii for the corresponding atoms.

Coulombic interactions were evaluated by assigning partial charges to O–C=O atoms, using bond moments of 0.74 D for C'–O and 2.3 D for C'=O.²⁴ Partial charges of −0.388, −0.113, and 0.501 ue for the oxygen of the carbonyl group, the ester oxygen, and the C' atom have been obtained, respectively. The apparent dielectric constant has been placed equal to 3.5.²⁴

The reported energy values refer to 1 mol of monomeric units.

Results and Discussion. Geometric and energetic aspects of our analysis can be summarized as follows.

The chain symmetry of PET in the crystalline state is *ti* with two centers of symmetry in the monomeric unit located at the center of the phenylene rings and at the center of the CH₂–CH₂ bonds. This leads us to consider one-half of a monomeric unit, coinciding with a structural unit. In the crystalline form of PET, with reference to Figure 5, the chains present θ₁ = −169.3°, θ₂ = 178.2°, and θ₃ = 158.7° and an identity period c = 10.75 Å,^{8,9} close to the value of the period of the chain in the highest extension (the last resulting in c = 10.83 Å under our geometrical assumptions).

The identity period of PET in the mesomorphic form is c = 10.3 Å, still not far from the length of a monomeric unit in the highest extension. In the following analysis of conformational energy and geometric features of PET chains, our goal is to find suitable ordered and disordered conformations leading to $c \approx 10.3$ Å, corresponding to local minima of conformational energy. The calculations of the conformational energy have been performed on a portion of PET chain like that shown in Figure 5, comprising two monomeric units. We have good reasons, as will be clear in the following, to suppose that this portion is sufficiently large to mimic the energy interactions of the whole polymeric chain, at least in the extended conformations of our interest.

Owing to the high number of geometrical parameters involved, besides the constancy of bond length and bond angles, the following simplifying assumptions have been made.

Dihedral angles θ_1 , θ_2 , and θ_4 have been placed equal to 180° (possible fluctuations not being included in the reported calculations). The other possible conformational minima (cis for θ_1 and θ_2 , gauche for θ_4) were not considered, since they generally cause bending of the chain backbone, with a too high shortening of the chain period as a result. For instance, calculations placing θ_4 in a gauche state show that for all possible variations of θ_3 and θ_3' the length of the monomeric unit l , defined as the distance between the centers of two consecutive phenylene rings, becomes too short (in particular, in the range $5 < l < 8.5$ Å). This simplifying assumption is also based on the fact that the known crystalline structures of several polyesters of the series $[\text{C}_6\text{H}_4\text{COO}(\text{CH}_2)_n\text{OOC}]_x$ ($n = 2, 3, \dots, 6$) always show these dihedral angles (θ_1 , θ_2 , and θ_4) in nearly trans conformations.⁹

The only dihedral angles left free in the reported calculations are θ_3 and θ_3' . As we shall see in the following, large deviations of these dihedral angles from the trans conformations are compatible with sufficiently extended chains. Moreover, such large deviations are observed in some crystalline structures of the above polyesters, like, for instance, in the α form of poly(butylene terephthalate), where $\theta_3 = -\theta_3' = 88^\circ$.^{9,16}

Figure 6 shows maps of the conformational energy and the length of the monomeric units, calculated by varying θ_3 and θ_3' . The continuous lines are loci of points (θ_3, θ_3') , with fixed values of the conformational energy (Figure 6A) and of the length of the monomeric units l (Figure 6B). Starred points on map 6A put in evidence local energy minima. In particular, the following have been found: (i) one absolute minimum (for which a zero energy has been assumed) with $\theta_3 = \theta_3' = 180^\circ$ and $l = 10.83$ Å; (ii) four relative minima (0.6 kcal/mol) centered at $\theta_3 = 180^\circ$, $\theta_3' = \pm 80^\circ$ and at $\theta_3 = \pm 80^\circ$, $\theta_3' = 180^\circ$, with $l = 10.4$ Å; (iii) two relative minima (1.2 kcal/mol) at $\theta_3 = \pm 80^\circ$, $\theta_3' = \mp 80^\circ$, with $l = 10.4$ Å; (iv) two relative minima (1.4 kcal/mol) at $\theta_3 = \pm 80^\circ$, $\theta_3' = \pm 80^\circ$, with $l = 10.0$ Å.

In summary, the eight conformers listed at points ii–iv show lengths of monomeric units not far from the experimental identity period of PET in the mesomorphic form. This is clearly shown by the dashed line in Figure 6A, which represents the locus of points (θ_3, θ_3') with $l = 10.3$ Å (taken from Figure 6B).

The possibility of building up polymer chains with a chain repetition c close to 10.3 Å with regular or random sequences of these minimum energy conformations will be the subject of our next analysis.

Regular sequences of all identical monomeric units produce identity periods c close to the experimental value in the mesomorphic form (10.3 Å) only for two of the minimum energy conformations of Figure 6A. In fact, this occurs for the conformations with $\theta_3 = \pm 80^\circ$ and $\theta_3' = \mp 80^\circ$ (case iii) which give rise to two fully equivalent polymer chains with symmetry ti . The other regular conformations, corresponding to the energy minima of kinds ii and iv, correspond to helical structures which may show unit heights much smaller than the length of the monomeric unit and very long identity periods.

The periodicity of polymer chains obtained by disordered successions of the minimum energy conformations previously described is close to 10.3 Å only if there is a nearly perfect alignment of successive monomeric units. As a parameter of the degree of alignment of the chain, we introduce the angle Ω , defined as the angle between the two segments joining the center of a phenylene ring to the centers of the two adjacent phenylene rings. Possible values of Ω are shown, as an example, for the case when

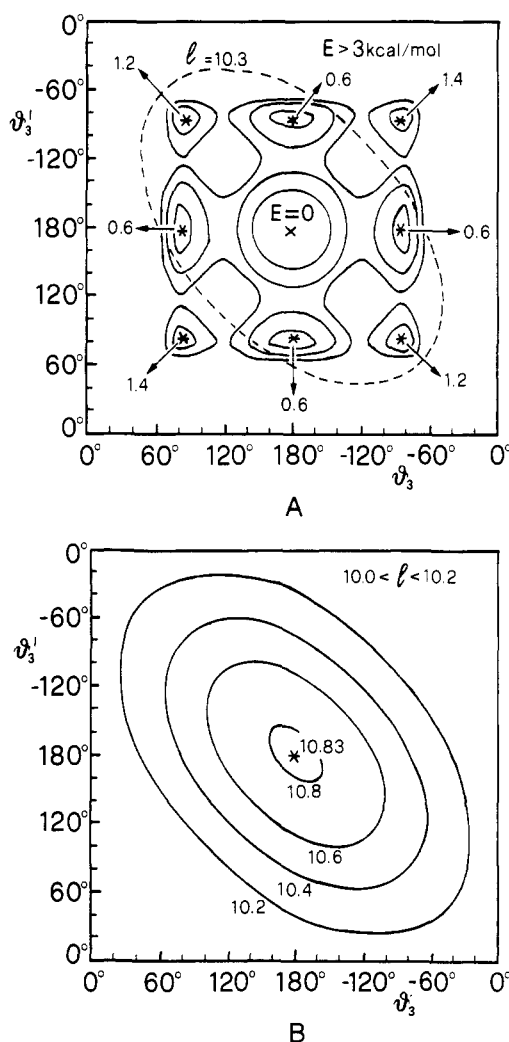


Figure 6. (A) Conformation energy map $E(\theta_3, \theta_3')$ of the dimer shown in Figure 5 for $\theta_1 = \theta_2 = \theta_4 = 180^\circ$. Contour lines with constant conformational energy are at regular intervals of 1.0 kcal/mol (per monomeric unit), starting from the absolute minimum located at $\theta_3 = \theta_3' = 180^\circ$; the energy values for the secondary minima are also indicated. (B) Map of the length of a monomeric unit $l(\theta_3, \theta_3')$ for $\theta_1 = \theta_2 = \theta_4 = 180^\circ$. The constant values of l (in Å) corresponding to the contour lines are indicated. The dashed line in (A) is the locus of points (θ_3, θ_3') with $l = 10.3$ Å.

the first monomeric unit is in the fixed conformation with $\theta_3 = +80^\circ$ and $\theta_3' = 180^\circ$, while the values of θ_3 and θ_3' in the successive monomeric unit are left free. Curves in Figure 7 represent loci of points (θ_3, θ_3') (of the second monomeric unit) for which Ω is constant. It is apparent that, even within our rigid geometrical assumptions, some sequences of conformations are well aligned (in this case, for instance, $\Omega = 180^\circ$ for the sequences of pairs of monomeric units with (θ_3, θ_3') values of the kind $(+80^\circ, 180^\circ)$ – $(180^\circ, -80^\circ)$ or $(+80^\circ, 180^\circ)$ – $(-80^\circ, +80^\circ)$). For the other sequences of the previously described minimum energy conformations Ω is always in the range 155 – 180° .

More generally, values of Ω lower than 149° are not obtained, within our geometrical assumptions, for whatever pair of the conformers corresponding to the conformational energy minima of Figure 6A (i–iv). This suggests that a fair degree of alignment of successive monomeric units can be easily obtained for such disordered sequences of monomeric units, if our arbitrary rigid constraints on the values of dihedral angles and/or bond angles are released, without a significant increase of the internal energy.

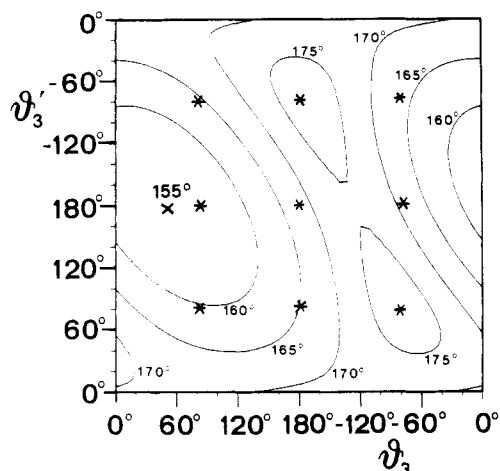


Figure 7. Map of the angle Ω between two segments joining the center of a phenylene ring to the centers of the two adjacent ones when $\theta_3 = +80^\circ$, $\theta_3' = 180^\circ$ in a first monomeric unit and θ_3, θ_3' are left free in the second monomeric unit ($\theta_1 = \theta_2 = \theta_4 = 180^\circ$). The values corresponding to the minimum and to the contour lines are indicated. The nine asterisks indicate the conformational energy minima of Figure 6A.

In conclusion, conformations of monomeric units in the regions of some or all of the nine minima of conformational energy of Figure 6A can be randomly joined together at a low cost of energy, giving rise to highly extended conformationally disordered polymer chains with an average identity period not far from 10.3 Å.

In these conformationally disordered polymer chains the angle between the planes of consecutive phenylene rings can assume all of the values comprised in the range $0-180^\circ$. This can be easily understood considering that (i) already within our geometric assumptions monomeric units with $\theta_3 = 180^\circ$, $\theta_3' = \pm 80^\circ$ or with $\theta_3 = \pm 80^\circ$, $\theta_3' = 180^\circ$ would place the plane of the two consecutive phenylene rings at $\pm 80^\circ$, while conformers with $\theta_3 = \theta_3' = \pm 80^\circ$ would place these planes at $\pm 20^\circ$ and (ii) distortions of bond and dihedral angles at the junctions between successive monomeric units as well as possible deviations of all the dihedral angles from the fixed assumed values are possible. It is worth recalling that, instead, the chains of PET in the crystalline form or, more generally, in all the regular conformations in the symmetry ti (monomeric units with $\theta_3 = -\theta_3'$) have their phenylene rings coplanar all along the chain.

It is worth noting that, although the numeric values of the energy differences and of the calculated geometrical parameters l and Ω depend on the exact values of the bond lengths, bond angles, and torsion angles, which were held fixed in the calculations, and on the energy parameters, no reasonable adjustment of these parameters can modify our conclusions.

Fourier Transform Calculations

Methods. Fourier transform calculations have been performed on isolated-chain models obtained by regular or disordered sequences of monomeric units in different conformations, as discussed before. The Fourier transform of isolated chains can be advantageously compared to the diffracted intensity far from the equator, with the assumption of the absence of rotational (around the chain axis) and translational (along the chain axis) order between adjacent parallel chains. Near the equator the comparison is, instead, less significant, since also interferences between adjacent chains should be accounted for.

The diffraction by fibers is conveniently expressed as a function of the reciprocal space cylindrical coordinates

ξ , Ψ , and ζ as

$$I(\xi, \Psi, \zeta) = F(\xi, \Psi, \zeta) F^*(\xi, \Psi, \zeta) \quad (5)$$

In eq 5 $F(\xi, \Psi, \zeta)$ is the structure factor of a single polymer chain and the asterisk denotes the complex conjugate. $F(\xi, \Psi, \zeta)$ can be developed in terms of the contributions of the atoms as

$$F(\xi, \Psi, \zeta) = \sum_{A=1}^r \left\{ \sum_{j=1}^n f_{A,j} \exp[2\pi i(\xi r_{A,j} \cos(\Psi - \varphi_{A,j}) + \zeta z_{A,j})] \right\} \exp(2\pi i \zeta z_A) \quad (6)$$

In eq 6 r is the number of monomeric units in a chain, n is the number of atoms per monomeric unit, $f_{A,j}$ is the atomic scattering factor of the j th atom in the A th monomer, $r_{A,j}$, $\varphi_{A,j}$, and $z_{A,j}$ are the cylindrical coordinates of the atoms in the monomeric unit, and z_A is the distance of the A th monomeric unit from the first one.

Since we are interested in the cylindrically averaged diffraction intensity of a single chain, eq 5 should be averaged over all possible values of Ψ in reciprocal space. This is conveniently done developing eq 6 in a series of Bessel functions^{25,26} as follows:

$$F(\xi, \Psi, \zeta) = \sum_{A=1}^r \left[\sum_{j=1}^n f_{A,j} \left(\sum_{m=-\infty}^{+\infty} J_m(2\pi r_{A,j} \xi) \exp\{i[m(\Psi + \pi/2) - m\varphi_{A,j} + 2\pi \zeta z_{A,j}]\} \right) \right] \exp(2\pi i \zeta z_A) \quad (7)$$

with J_m and m th-order Bessel function. After substitution of eq 7 in eq 5 and integration of the resulting formula over Ψ from 0 to 2π , one obtains (dividing the result of the integration by 2π)

$$I(\xi, \zeta) = \sum_{A=1}^r \sum_{B=1}^r \left\{ \sum_{i=1}^n \sum_{j=1}^n f_{A,j} f_{B,i} C_{A,j,B,i} \cos[2\pi \zeta(z_{A,j} - z_{B,i})] \right\} \cos[2\pi \zeta(z_A - z_B)] \quad (8)$$

where j and i are the indices of the atoms in the A th and B th monomeric units, respectively. In eq 8 $C_{A,j,B,i}$ is given by

$$C_{A,j,B,i} = 2 \sum_{m=1}^{\infty} J_m(2\pi r_{A,j} \xi) J_m(2\pi r_{B,i} \xi) \cos[m(\varphi_{A,j} - \varphi_{B,i}) + J_0(2\pi r_{A,j} \xi) J_0(2\pi r_{B,i} \xi)] \quad (9)$$

Equation 8 gives the formula used in our calculations for the diffraction intensity of isolated polymer chains (the Debye factor was not included). Fourier transform calculations were generally performed on polymer chains of 20 monomeric units (280 atoms in total). The resulting chain exhibits a total length of 200 Å, well above the coherent length of 80 Å established on the basis of experimental data (see Experimental Section). This choice is due to the fact that chains made of eight monomeric units (80 Å) give rise at small values of the diffraction angle to spurious effects because of the termination of the chain. This produces only a slightly narrowing of the peaks along ζ and, of course, does not change the general conclusions which can be drawn. Calculations were performed in reciprocal space in the range $0 < \xi < 0.6 \text{ Å}^{-1}$ at intervals of 0.01 units and $0 < \zeta < 0.6 \text{ Å}^{-1}$ at intervals of 0.005 units. Calculated diffraction intensity has not been reported for values of $(\zeta^2 + \xi^2)^{1/2} \leq 0.07 \text{ Å}^{-1}$ (chain termination effect present). In the case of irregular chains, the reported maps are obtained by averaging the calculated $I(\xi, \zeta)$ for at least ten different chain models.

Results and Discussion. The calculated diffraction intensity $I(\xi, \zeta)$ for isolated model chains is compared to

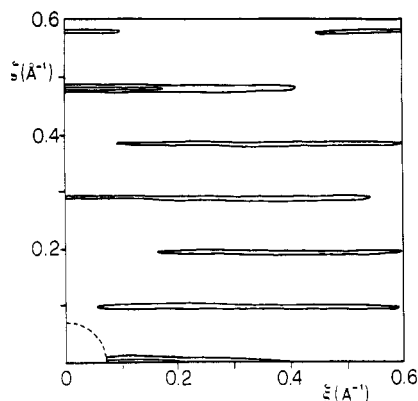


Figure 8. Decimal logarithm of the calculated diffraction intensity $I(\xi, \zeta)$ for a regular chain of PET with all the monomeric units with $\theta_3 = -\theta_3' = 80^\circ$ vs the reciprocal coordinates ξ and ζ . Contour lines correspond to $\log [I(\xi, \zeta)]$ equal to 3 and 2.25, $\log [I(0, 3/c)]$ being placed equal to 3.

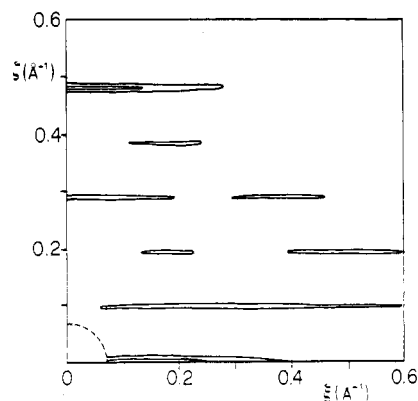


Figure 9. Decimal logarithm of the calculated diffraction intensity $I(\xi, \zeta)$ for a slightly irregular chain (see text) vs the reciprocal coordinates ξ and ζ . Contour lines correspond to $\log [I(\xi, \zeta)]$ equal to 3 and 2.25, $\log [I(0, 3/c)]$ being placed equal to 3.

the experimental diffraction pattern of PET in the mesomorphic form. In particular, we aim at reproducing the complete absence of layer lines (both crystalline reflections and diffuse halos) out of the meridian and the position and the intensity ratio of the diffraction intensity maxima along the meridian.

In the case of regular model chains, strong diffuse maxima are always present on layer lines. This is shown, for instance, in Figure 8, which represents the calculated diffraction intensity $I(\xi, \zeta)$ for a regular chain in the *ti* symmetry having all monomers with $\theta_3 = -\theta_3' = \pm 80^\circ$ ($c = 10.4$ Å).

Well-defined layer lines are present also for conformationally disordered chains, when disorder is not sufficiently high. Let us consider, for instance, conformationally disordered chains, obtained following the arbitrary rule of putting in sequence only monomeric units (corresponding to the conformational energy minima of Figure 6A) leading to $\Omega = 180^\circ$ without relaxing our geometrical constraints ($\theta_1 = \theta_2 = \theta_4 = 180^\circ$, $\theta_3, \theta_3' = \pm 80^\circ$ or 180°). The calculated diffraction intensity is shown in Figure 9. These chain models still present strong correlations between the planes of the phenylene rings along the chain (they all lie in only three planes containing the chain axis).

Let us consider now more disordered model chains obtained by random sequences of all nine minimum energy conformers. Obviously, resulting chains are not generally straight. As discussed in a previous section, the obtainment of straight chains, which is of course necessary for

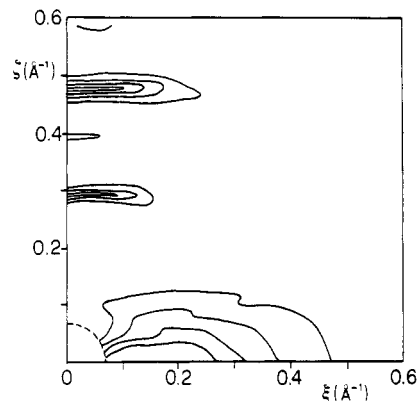


Figure 10. Decimal logarithm of the calculated diffraction intensity $I(\xi, \zeta)$ for an irregular chain obtained putting in sequence monomeric units in all of the nine minima of the conformational energy of Figure 6A vs the reciprocal coordinates ξ and ζ . Contour lines correspond to $\log [I(\xi, \zeta)]$ equal to 3.0, 2.75, 2.5, and 2.25, $\log [I(0, 3/c)]$ being placed equal to 3.

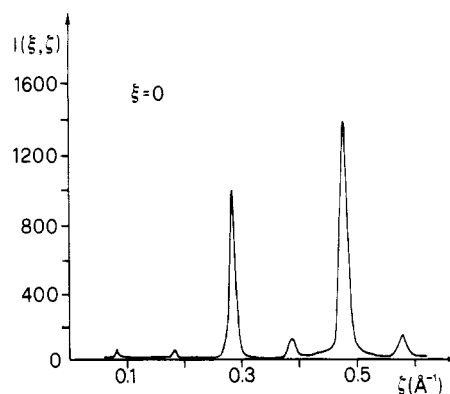


Figure 11. Plot along the meridian ($\xi = 0$) of the calculated diffraction intensity of Figure 10.

the packing, can be assured by small variations of dihedral and bond angles. However, for the sake of simplicity, in the model chains our rigid geometrical constraints were maintained and, to ensure their substantial straightness, only chains (obtained by nearly random sequences of different conformers) with mean periodicity greater than 10.2 Å were taken into consideration. This simplifying calculation procedure, although reducing the randomness in the sequence of the conformers, still allows for a high degree of conformational disorder in the chains and removes any long-range correlation between the planes of the phenylene rings.

The diffraction intensity map $I(\xi, \zeta)$ for chain models obtained by nearly random sequences of all nine considered conformers is reported, for instance, in Figure 10. Figure 11 displays the calculated diffraction intensity along the meridian. The absence of layer lines off the meridian (Figure 10), the correct positions of the meridional reflections, and their qualitative intensity pattern (Figure 11) compare well with the main features of the experimental patterns of Figures 3 and 4. These are good indications that the proposed conformationally disordered model chains are possibly not far from those present in the mesomorphic form of PET. The intensity ratio between the meridional reflections at $\zeta = 3/c = 0.29$ Å⁻¹ and $\zeta = 5/c = 0.48$ Å⁻¹ is not satisfactory, however. This ratio can be only partially improved by discarding some of the cited minimum energy conformations (in particular, the conformations of kinds i and iv). To get a better agreement for this intensity ratio, a more accurate analysis is in progress in our laboratories, where the assumed rigid geometrical constraints for the chain models are reduced.

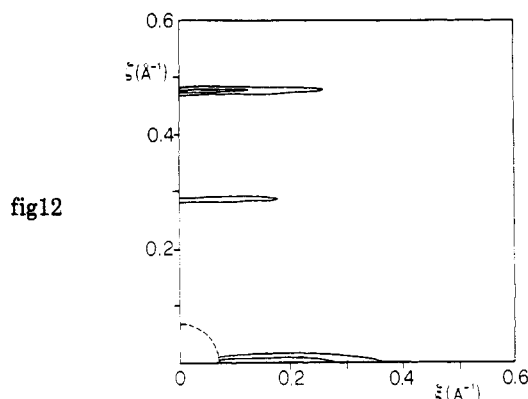


Figure 12. Decimal logarithm of the calculated diffraction intensity $I(\xi, \zeta)$ vs the reciprocal coordinates ξ and ζ for a more simplified model simulating random sequences of perfectly aligned conformers (see text). Contour lines correspond to $\log [I(\xi, \zeta)] = 3$ and 2.25 , $\log [I(0, 3/c)]$ being placed equal to 3 .

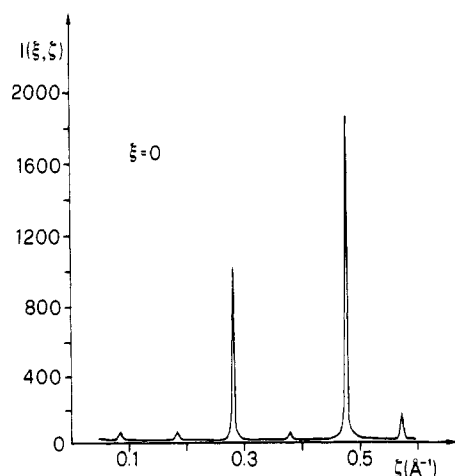


Figure 13. Plot along the meridian ($\xi = 0$) of the calculated diffraction intensity of Figure 12.

In summary, the comparison between the present Fourier transform calculations and the experimental diffraction data suggests that the chains in the mesomorphic form present a disordered sequence of extended minimum energy conformations, possibly close to those corresponding to the calculated minimum energies. We recall that in these models there is no long-range correlation between the planes of the phenylene rings along the chain.

It is possibly also worth mentioning an even more simplified model which qualitatively accounts for the observed diffraction pattern of the mesomorphic form, since it contains the essential features of the discussed models. In this case, the model chains simulate random sequences of perfectly aligned conformers by averaging the structure factor contribution of each monomeric unit over all possible orientations and conformations. The method of calculation of the diffraction intensity is reported in the Appendix. This model is less realistic, since it does not present acceptable chemical bonds between successive monomeric units. Figures 12 and 13 report, as an example, the (ξ, ζ) map and the plot along the meridian, respectively, of the calculated diffraction intensity in the case of model chains built up taking all nine minimum energy conformers.

Almost the same results can be obtained even if only one of the conformers of suitable length of kind ii or iii is taken into consideration. This is a further indication that the presence of random rotations along the chain axis of the planes including the phenylene rings is very relevant for the model.

As a final remark, we note that, according to our analysis, the tilting of the chain axis from the fiber axis⁴ is unnecessary to account for the observed diffraction pattern of the mesomorphic form. This could suggest that this tilting in crystalline PET⁸ would occur not in the orientation process but upon crystallization.

Conclusions

The reported Fourier transform calculations of isolated-chain models indicate that the experimental diffraction pattern of the mesomorphic form of PET can be qualitatively accounted for by extended linear chains obtained by random sequences of monomeric units in different minimum energy conformations. This indicates a substantial absence of rotational (around the chain axis) and translational (along the chain axis) order between adjacent parallel chains.

The present energy and geometrical analyses suggest that these conformers could be characterized by all nearly trans conformations, but for the $C'-O-C-C$ (θ_3 and θ_3') dihedral angles, for which, besides values close to 180° , values close to $+80^\circ$ and -80° would be possible.

These random sequences of monomeric units generate chains in which any long-range correlation between the planes of the phenylene rings along the chain is absent.

Acknowledgment. This work was supported by the Ministero dell'Università e della Ricerca Scientifica e Tecnologica (Italy) and by the Consiglio Nazionale delle Ricerche. X-ray diffraction data were recorded with a Nonius CAD4 automatic diffractometer (Centro Interdipartimentale di Metodologie Chimico Fisiche, University of Naples).

Appendix

This method is a straightforward application of the unidimensional paracrystalline theory (see ref 27) and leads to a very simple formula for the diffraction intensity. Indeed, following ref 28, Chapter 4, pp 146–149 (and also ref 27), the latter for a chain of degree of polymerization r is

$$I(\xi, \zeta) = \langle f \rangle^2 L^2(\zeta) + r(\langle f^2 \rangle - \langle f \rangle^2) \quad (A-1)$$

where $L(\zeta)$ is the Laue factor for an ideal linear crystal of r unit cells, $\langle f \rangle^2$ is the square of the structure factor of the monomeric unit for each ξ, ζ averaged over all possible orientations around the chain axis of the considered conformations, and $\langle f^2 \rangle$ is the corresponding mean square structure factor per monomeric unit.

References and Notes

- (1) Bonart, R. *Kolloid-Z.* **1966**, *213*, 1.
- (2) Bonart, R. *Kolloid-Z.* **1966**, *210*, 16.
- (3) Bonart, R. *Kolloid-Z.* **1968**, *231*, 438.
- (4) Asano, T.; Seto, T. *Polym. J.* **1973**, *5*, 72.
- (5) Hinrichsen, G.; Adam, H. G.; Krebs, H.; Springer, H. *Colloid Polym. Sci.* **1980**, *258*, 232.
- (6) Napolitano, M. J.; Moet, A. *J. Appl. Polym. Sci.* **1987**, *34*, 1285.
- (7) Fakirov, S.; Evtatiev, M. *Polymer* **1990**, *31*, 431.
- (8) Daubeny, R. P.; Bunn, C. W.; Brown, C. J. *Proc. R. Soc. London* **1954**, *A226*, 531.
- (9) Hall, I. H. In *Structure of Crystalline Polymers*; Hall, I. H., Ed.; Elsevier Applied Science Publishers: London, 1984; Chapter 2, p 39.
- (10) Lindner, W. L. *Polymer* **1973**, *14*, 9.
- (11) Lemanska, G.; Narebska, A. *J. Polym. Sci., Polym. Phys. Ed.* **1980**, *18*, 917.
- (12) Deopura, B. L.; Kumar, V.; Sinha, T. B. *Polymer* **1977**, *18*, 856.
- (13) Sun, T.; Zhang, A.; Li, F. M.; Porter, R. S. *Polymer* **1988**, *29*, 2115.
- (14) Perez, S.; Brisse, F. *Can. J. Chem.* **1975**, *53*, 3551.

- (15) Perez, S.; Brisse, F. *Acta Crystallogr.* **1976**, *B32*, 470.
- (16) Yokouchi, M.; Sakakibara, Y.; Chatani, Y.; Tadokoro, H.; Tanaka, T.; Yoda, K. *Macromolecules* **1976**, *9*, 266.
- (17) Sundararajan, P. R.; Labrie, P.; Marchessault, R. H. *Can. J. Chem.* **1975**, *53*, 3557.
- (18) Vacatello, M.; Flory, P. J. *Macromolecules* **1986**, *19*, 405.
- (19) Tonelli, A. E. *J. Polym. Sci., Polym. Lett. Ed.* **1973**, *11*, 441.
- (20) Ooj, T.; Scott, R. A.; Vanderkooi, G.; Scheraga, H. A. *J. Chem. Phys.* **1967**, *46*, 4410.
- (21) Yoon, D. Y.; Suter, U. W.; Sundararajan, P. R.; Flory, P. J. *Macromolecules* **1975**, *8*, 784.
- (22) Bondi, A. *J. Phys. Chem.* **1964**, *68*, 441.

- (23) Yoon, D. Y.; Sundararajan, P. R.; Flory, P. J. *Macromolecules* **1975**, *8*, 776.
- (24) Sundararajan, P. R.; Flory, P. J. *J. Am. Chem. Soc.* **1974**, *96*, 5025.
- (25) Chivers, R. A.; Blackwell, J. *Polymer* **1985**, *26*, 997.
- (26) Biswas, A.; Blackwell, J. *Macromolecules* **1988**, *21*, 3146.
- (27) Hosemann, R.; Bagchi, S. N. *Direct Analysis of Diffraction by Matter*; North-Holland Publishing Co.: Amsterdam, 1962.
- (28) Tadokoro, H. *Structure of Crystalline Polymers*; J. Wiley & Sons: New York, 1979.

Registry No. PET, 25038-59-9.